

RESEARCH HIGHLIGHTS

Polydopamine Modified Biomimetic Gold Nanoparticles for Dual Photothermal Therapy

Su Zhiming¹ Hem Sagar Rim^{2*}

1. China Medical Medicine Institute, Beijing, 100000, China;

2. Medicine, Nepal Health Research Council, 44601, Nepal

*Correspondence Author: Hem Sagar Rim, Medicine, Nepal Health Research Council, 44601, Nepal, Email: HSR@yahoo.com.

Abstract: Our study produced Polydopamine modified gold nanoflowers with controlled morphology for anti-tumor photothermal therapy. The branch structure contains abundant (Au NFs). By adjusting the reduction rate, the dosage of reducing agent (sodium borohydride) and the reduction temperature, we can adjust the morphology and particle size of Au NFs. We found that the lower reaction temperature is, the more abundant the surface branching structure of gold nanoflowers is, by adjusting the reaction temperature. and the largest specific surface area of golden nanopowder was found at 0 °C. The results of TEM indicated that with the increase of sodium borohydride, the diameter of gold nano flowers gold nanoflowers decreased and was in the range of 60~100nm, and it has good EPR effect After that, we modify poly (dopamine) (PDA) biomimetic layer on the surface of golden nanoparticles to obtain Au NFS@PDA. Poly (dopamine) has the ability, of photothermal conversion, which can enhance the plasma resonance ability and biocompatibility of gold nanoflowers in the near infrared region. We can control the thickness of polydopamine layer on the surface of gold nanoflowers between 7~15nm by adjusting dopamine DA concentration gold nanoflowers. Au NFS@PDA was characterized by its morphology and physical properties. We detect (UV-Vis) spectra in the near infrared region. And it showed obvious absorption peaks in the near infrared region of 575~650nm. Under the 808nm irradiation laser, the photothermal conversion of gold nanoflowers and polydopamine can be rapidly increased to 57°C. Fourier Transform Infrared Absorption Spectroscopy (FTIR) and X-ray Diffraction (XRD) analysis showed that polydopamine was modified successfully, Au NFS@PDA and Au NFs had no obvious difference in crystal form. The cell viability test showed that the bionic Au NFS@PDA had good biocompatibility and showed good antitumor activity against HeLa cells under NIR irradiation. The cell viability was only 12%. Therefore, we can use Au NFS@PDA with good biocompatibility as a promising photothermal conversion agent in tumor therapy.

Keywords: gold nanoflowers; Polydopamine; Template-free method; Controllable; Photothermal therapy

Received: 24th September 2020; **Accepted:** 12th October 2020; **Published Online:** 20th October 2020

1 Introduction

According to World Health Organization statistics, the rate and mortality rate of cancer incidence are rising year by year, which seriously threaten human life safety [1]. Photothermal therapy becomes a new effective treatment. The heat resistance of tumor cells is poor compared with

normal cells. When the temperature of photothermal conversion agent reaches 42-50 °C, it can cause the irreversible damage of tumor cells. At the same time, the normal tissue will not be damaged. It is a treatment with clinical potential [2-3].

Gold nanomaterials have the optical properties, that

is, local surface plasmon resonance (LSPR), which make them have the ability of strong light absorption and scattering. When light is irradiated on gold nanoparticles, the free electrons of metals quickly perceive the magnetic field, and the cations with the same incident light frequency begin to vibrate collectively, then the absorbed light energy can be converted to thermal energy rapidly [4-7]. When the ratio of length to width of gold nanoparticles increases, the maximum absorption spectrum will change to the near infrared region, which can be used in the photothermal treatment of cancer [8-9]. Among them, (Au NFs) as a kind of nanoparticles which has similar branching structure, has larger specific surface area and higher reaction activity, It is often used as antitumor photoheaters. At present, we mainly use template method as the synthesis method of Flos Lonicerae, which can regulate the morphology and particle size of Flos Lonicerae by adding polypeptide, protein or surfactant. For example, Han et al used (C18N3) as template to synthesize a kind of large-sized hollow golden nanoparticles, which showed good biocompatibility and good anti-tumor ability in 808nm radiation [10]. However, by reducing agent sodium borohydride or sodium borohydride, nano-flowers were directly reduced. For example, Mao et al reduced chloric acid to obtain gold nanoflowers by using hydroxylamine hydrochloric acid. Template-free preparation of the gold nanoflowers is more convenient and faster, and the nano-flowers we got showed good biological safety without post-treatment [11]. But in fact, it is not suitable to be used as drug carrier because of its poor biocompatibility, difficult to double biological metabolism and toxic side effects. Therefore, it is urgent to design bionic golden nanoparticles to increase their conversion potential in clinical applications.

Poly (dopamine) (PDA) is a main photo responder which has good photothermal conversion effect under near infrared irradiation [12]. Under alkaline condition, coating on the surface of various materials, dopamine can be polymerized to form poly (dopamine) (PDA). The formed PDA coating has a huge number of hydrophilic hydroxyl and amino functional groups which can improve the hydrophilicity of the materials and can also promote the adhesion of the cells with good biocompatibility [13-15]; At the same time, near infrared region is the maximum absorption wavelength of polydopamine, thus good photothermal conversion ability, which can enhance the surface plasmon resonance effect of precious metal nanoparticles [16-19].

Therefore, the study used template-free method to achieve the regulation of gold nanoflower flowers morphology and particle size by adjusting reaction temperature and reducing agent dosage. Furthermore, we prepared poly (dopamine) modified gold nanoparticles (Au NFs@PDA) by poly (dopamine) modified polydopamine, which taked advantage of low toxicity, stability and good biocompatibility. And we controlled the coating thickness by adjusting the concentration of dopamine. Finally, the photothermal transformation experiments showed that Au NFs@PDA had a strong photothermal transformation heating effect, and the cell survival rate proved that Au NFs@PDA had a good biological safety and anti-tumor ability, which demonstrated its application.

2 Experiment Reagent and Methodology

2.1 Experimental Equipment

Evolution300 (UV-Vis) Spectrophotometer, Thermo-Scientific, USA; Omni Nano-particle/Zeta Potentiometer, Brookhaven, USA; TecnaiG2spiritBiotwin Bio-Transmission Electron Microscope (TEM), -1FEI, USA; Nicolet6700 Fourier Transform Infrared Spectrometer (FTIR), ThermoFisher, USA; 3kW/*D8ADVANCEDaVinci multi-function X-ray diffractometer, Bruker, Germany; Elx800, BioTek, USA; Ti125 Infrared Camera, Fluke, USA; FC-808-5000-MM 808nm Laser, Shanghai Binzaki Technology Co, Ltd.

2.2 Experiment Reagent

(HAuCl₄•4H₂O), sodium borohydride, potassium carbonate (K₂CO₃), Tris- HCl, dimethyl sulfoxide (DMSO) and dopamine hydrochloride were purchased from Sinopharm Chemical Reagent Co, Ltd. Thiazolam (MTT) was purchased from Sigma-Aldrich; Cell culture medium (DMEM), fetal bovine serum (FBS) and phosphate buffer (PBS, pH=7.4) were purchased from Life Technologies. HeLa cells were purchased from Shanghai Institute of Cells, Chinese Academy of Sciences;

2.3 Experimental Methods

Preparation of golden nanoparticles Dissolve 1 mL of 1% chloric acid in 100 mL of ultrapure water, while stirring add 50 μL of sodium borohydride solution (5 mmol/L), and mix well. After 5 min, add 4mL NH₂OH•HCl (10 mmol/L) rapidly, and stir the mixture for 10 min. After centrifugation with high speed centrifuge (8000 r/min) for 5 min, remove the supernatant and the wash the precipitate with ultrapure water for 3 times to obtain golden nanoparticles. At 0°C, adjust the dosage of sodium

borohydride to 30, 70 and 90 μL respectively and detect the new height and particle size change of the samples control the reaction temperatures to 10, 20, 30 and 40 $^{\circ}\text{C}$, respectively, without other changes.

Preparation of Au NFs@PDA Disperse 20 μL golden nanoparticles in 10 mL Tris-HCl buffer (pH=8.5), add 2 mL dopamine solution (0.5 mg/mL), and then centrifuge at 8000 r/min for 10 min after 2 h reaction under magnetic stirrer, remove the supernatant and wash the precipitate with ultrapure water, centrifuge for 3 times. Adjust the concentration of dopamine solution to 1 and 2 mg/mL, and the other conditions remained unchanged.

Photothermal performance experiment Irradiate different samples with 808 nm laser (1W/cm²), and record thermal infrared images of ultrapure water and Au NFs@PDA group at 1, 2, 3, 4 and 5 min after laser irradiation.

Cytotoxicity experiment We evaluate the anti-tumor performance, according to the cell survival rate of the cells after treatment with different samples in the standard MTT experiment. The cells growing in logarithmic phase were inoculated in 96-well plates. The density of the cells was about 4×10^4 cells per well. After 24 h, add 50 μL per well of Au NFs@PDA solution at concentrations of 10, 50, 100, 250, 500 and 1000 $\mu\text{g}/\text{mL}$ respectively to 6 holes, to make the final concentrations of the samples 2, 10, 20, 50, 100 and 200 $\mu\text{g}/\text{mL}$. After 12h in incubator, continuously irradiate each hole in 808nm laser (1W/cm²) for 10 min, then incubate for 36 h. Wash the cells twice with PBS buffer, Add 200 μL medium and 20 μL 5 mg/mL MTT to each well, aspirate after 3~4 h incubation. Add 200 μL DMSO each well, and detect the absorbance at 490 nm. The cytotoxicity was not irradiated by laser, and the others are similar to the above-mentioned processes [20]. The formula calculates the corresponding cell survival rate:

$$\text{Cell survival rate (100\%)} = (\text{OD value of sample group} / \text{continuous OD value}) \times 100$$

3 Results and discussion

3.1 Effects of Reducing Agent Sodium Borohydride on the Diameter of Gold Nanoflowers

The synthesis of gold nanoparticles was realized by two steps. First, prepared gold seeds by reduction of sodium borohydride to Au, and then gold particles were grown by reduction of $\text{NH}_2\text{OH}\cdot\text{HCl}$ to Au^{3+} to form gold nanoparticles on gold seeds. It is reported that it can affect the particle size of synthesized golden nanoparti-

cles by influencing the unit concentration shadow of gold seed according to the concentration of reducing agents [21-22]. As shown in FIG. 2 and FIG. 3 (A), the diameter of the prepared flowers is in the range of 60~100nm, and with the increase of the concentration of sodium borohydride the diameter of the flowers decreases gradually. This is because the higher the concentration of sodium borohydride during the reduction, the more gold seeds are produced, the smaller the amount of chloric acid involved in the growth reaction of gold seeds, the smaller the diameter of golden nanoparticles. As shown in FIG. 3 (B), the zeta potential on the surface of four kinds of gold nanoflowers is $(-23.94 \pm 1.69) \sim (-25.01 \pm 2.11)$ mV. During the reduction process, the gold nanoparticles were negatively charged due to the adsorption of Cl^- in $\text{NH}_2\text{OH}\cdot\text{HCl}$. Subsequently, UV-Vis absorption spectra were used to detect the absorption spectra of golden nanoparticles (Figure 3C). The maximum absorption wavelength of the flower is less than 616 nm and blue shift occurs when the amount of sodium borohydride in the reaction system is more than 40 μL . The maximum absorption wavelength is 616 nm and the red shift occurs when the amount of sodium borohydride is less than 40 μL .

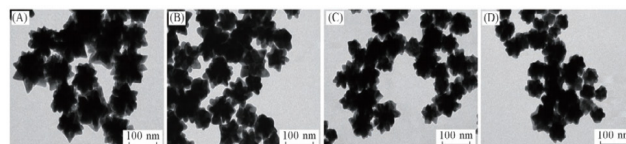


Fig.1 TEM images of Au NFs synthesized with different amounts of NaBH_4 , (A) 30; (B) 50; (C) 70; (D) 90; V (NaBH_4) / μL

3.2 Effects of Temperature on the Morphology of Gold Nanophyll

The reaction temperature is one of the important factors which influenced the morphology and particle size of golden nanoparticles. As shown in the TEM photo (2A-E), The morphology of Au NFs changed from rough surface to smooth surface, small branches and even disappeared nanoparticles when the incubation temperature was 0°C - 40°C . At 30 and 40°C , the branching structure of Au NFs surface almost disappeared and the particle size increased. This is due to the diffusivity of the reducing agent at different temperatures. When the temperature was lower, the diffusion rate of the active species of gold atom produced by Au^{3+} reduction in the solution was slower, which resulted in the formation of gold nanoparticles with rich branching structure. When the temperature rised, the diffusion rate of Au^{3+} in the

solution increased, and the reaction rate with reducing agent increased, thus it accelerated the reduction growth of gold on the surface of gold seed, which formed gold nanoparticles [23] with larger diameter and smoother surface.

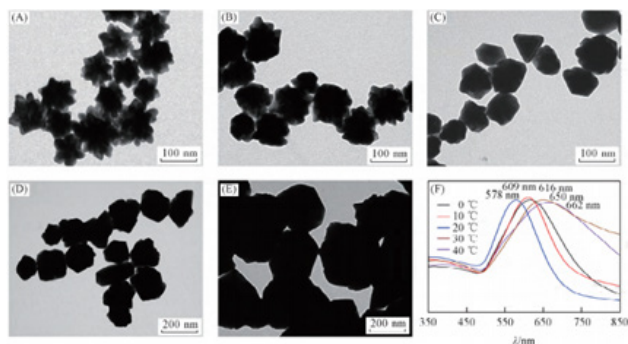


Fig.2

3.3 Characterization of Polydopamine Modified Gold Nano-flowers

As shown in Figure 3-3A, a core-shell Lan-Au NFs@PDA nanocomposite with a thickness of about 15 nm was formed after PDA spontaneous deposition on the surface of Lan-Au NFs.

According to the richness of the maximum absorption wavelength and branch, Select Au NFs prepared with 20 μL sodium borohydride at 0°C as the representative (Au NFs20). Firstly, Expressed PDA-Au NFs prepared by reaction of Au NFs20 with 1,2 and 5 mg/mL dopamine solution as PDA-Au1, PDA-Au2 and PDA-Au5, respectively. And then they were subsequently characterized by infrared spectroscopy, as shown in Figure 4(A). In contrast, we observed the absorption peaks at 1285 and 1500 cm^{-1} of polydopamine-modified golden nanoparticles. The former could be attributed to the absorption of aromatic rings on PDA and the latter to the bending vibrations of N-H bonds on PDA. Figure 4 (B) XRD pattern shows that there are five diffraction peaks for Au NFs20 and PDA-Au5, at 38.28°, 44.56°, 64.77°, 77.84° and 81.93° respectively. Which can be attributed to the crystal structure of (111), (200), (220), (311) and (222) of gold at, and indicates that it is a cubic crystal structure with face center. The particle size of Au NFs20 is 78.76nm by Scherrer formula, which has an error compared with the particle size of about 100 nm of Au NFs20 in the TEM picture shown in Fig. 5 (A), due to the fact that Au NFs is not a uniform sphere.

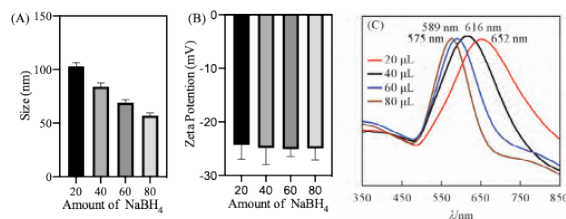


Fig.3 Hydrodynamic diameter (A) , zeta potential (B) and UV-Vis spectra (C) of AuNFs synthesized with 20 , 40 , 60 and 80 μL .

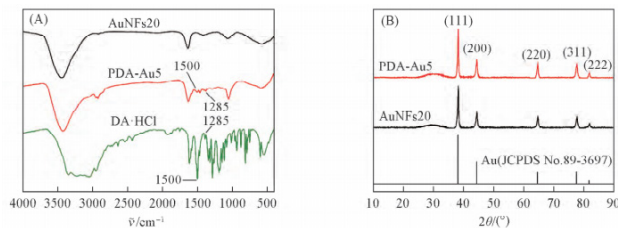


Fig.4 FTIR spectra of AuNFs prepared with 20 μL AA (AuNFs20) , AuNFs modified with 5 mg/mL DA · HCl (PDA-Au5) and DA · HCl (A) and XRD patterns of standard Au (JCPDS No. 89-3697) , AuNFs20 and PDA-Au5 (B)

Subsequently, TEM was used to characterize the thickness of PDA-Au NFs. FIG. 5 (A) ~ (D) show the TEM images of Au NFs20, PDA-Au1, PDA-Au2 and PDA-Au5, respectively. As can be seen from the figure, the morphology of the gold nanoflowers was almost unchanged after modification. The thickness of PDA-Au1, PDA-Au2 and PDA-Au5 corresponding to PDA-Au1, PDA-Au2 and PDA-Au5 were 8.7, 9.3 and 14.2 nm respectively when the concentration ratio of dopamine solution is 1 : 2 : 5. It shows that as the concentration of DA solution increased, the thickness of the formed PDA gradually increased. According to the results in Figure 6(A), it can be seen that after Au NFs20 is modified by polydopamine, PDA will enhance the hydrophilicity of the material, and the hydrated particle size will also increase. As shown by the zeta potential in Figure 6 (B), the potentials of PDA-Au1, PDA-Au2 and PDA-Au5 are negative due to the deprotonation of phenolic hydroxyl groups in PDA. FIG. 6 (C) shows the UV-visible spectra of Au NFs20, PDA-Au1, PDA-Au2 and PDA-Au5. The corresponding maximum absorption wavelengths are 652, 692, 704 and 737nm, respectively. Obviously, the thicker the polydopamine layer was, the more obvious the red shift of the maximum absorption wavelength was. This red shift phenomenon is due to the existence of the polydopamine layer, which increases the extinction and scattering cross-section of the golden nanoflowers, further improves the refractive index, thus enhances the plasma resonance effect of the golden nanoflowers, thus promotes the near infrared absorption of the golden nanoflowers [24].

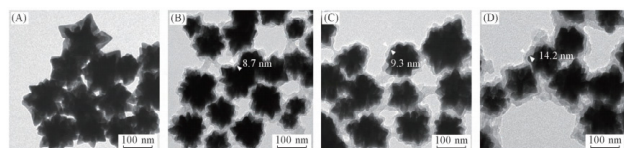


Fig.5 TEM images of AuNFs20 (A), PDA-Au1 (B), PDA-Au2 (C) and PDA-Au5 (D)

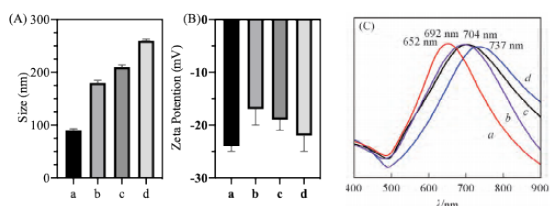


Fig.6 Hydrodynamic diameters (A), zeta potentials (B) and UV-Vis spectra (C) of AuNFs 20 (a), PDA-Au1 (b), PDA-Au2 (c) and PDA-Au5 (d)

3.4 Photothermal Conversion Performance Testing

FIG. 7 (A) shows the photothermal conversion of different samples irradiated with 808nm laser ($1\text{W}/\text{cm}^2$) for 10 min. As shown in the temperature-time curve of Figure 7(B), the temperature of ultrapure water had no obvious change, while the temperature of Au NFs group risen by 13.3°C and that of PDA-Au5 group risen by 29.4°C , the highest temperature was 57°C , which indicated that PDA have effective capability of enhancing the photothermal conversion of gold nanoflowers.

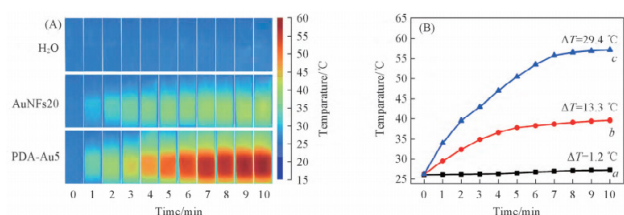


Fig.7 Thermal images (A) and temperature-time profiles (B) of H_2O (a), AuNFs20 (b) and PDA-Au5 (c) under irradiation of 808 nm laser ($1\text{W}/\text{cm}^2$) for 10 min

3.5 MTT Experimental Analysis

We use MTT assay to evaluate the cytotoxicity of Au NFs20 and PDA-Au5 cultured in vitro for 48 h. As shown in Figure 8 (A), the cell survival rate decreased, and the cell survival rate was about 75% at $200\ \mu\text{g}/\text{mL}$ as the concentration of Au NFs20 increased from $5\ \mu\text{g}/\text{mL}$ to $200\ \mu\text{g}/\text{mL}$. Compared with the same concentration of PDA-Au5, the cell survival rate reached nearly 90%. Obviously, PDA improves the biocompatibility of gold nanoflowers. In the photothermal treatment group shown in Figure 8 (B), the cell survival rate significantly reduced, with only 30% at $200\ \mu\text{g}/\text{mL}$ Au NFs20. By contrast the cell survival rate was about 10% at the same concentration of PDA-Au5, indicating a significant increase in PDA-

modified Au NFs photothermal conversion and enhanced antitumor activity.

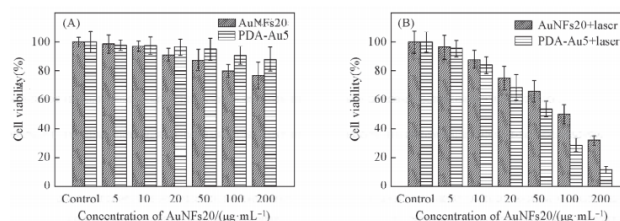


Fig.8 Cytotoxicity of HeLa cells cultivated with AuNFs and PDA-Au5 without (A) or with (B) a 10 min laser ($1\text{W}/\text{cm}^2$)

4 Conclusion

Gold nanoparticles with controllable morphology and size, and rich branch structures were prepared by template-free method. The lower reaction temperature is, the more abundant branching structure of gold nanoflowers we can get, among which 0°C is the best reaction temperature. The more we use sodium borohydride, the smaller the diameter of golden nanoparticles is. The maximum change is in the range of $60\sim 100\ \text{nm}$, and the maximum absorption wavelength is in the range of $575\sim 650\ \text{nm}$. PDA improved the absorption wavelength of Au NFs to $650\sim 740\ \text{nm}$ in near infrared region. At the same time, with the concentration of DA in solution, the thickness of PDA layer increased, the maximum thickness of PDA layer can reach about 14nm . After irradiation with 808 laser, the temperature of PDA-Au NFs solution risen to 57°C in 10 minutes. MTT experiment showed that PDA modified materials had low cytotoxicity, good biocompatibility and strong cytotoxicity to tumor cells under laser irradiation, which indicated that polydopamine modified golden nanoparticles had potential application prospect in photothermia biomedical field.

References

- [1] Jia W. F., Li J. R., Lin G. H., Jiang L., Cryst. Growth. Des., 2011, 11(9): 3822—3827
- [2] Li S. N., Zhang L. Y., Wang T. T., Li L., Su Z. M., Chem. Commun., 2015, 51(76): 14338—14341
- [3] Wang C. R., Yan X. Z., Yu Y. F., Mater. Res. Innov., 2014, 18(Sup2): 585—590
- [4] Ong X. Y., Chen S., Nabavi E., Regoutz A., Payne D. J., Elson D. S., Dexter, D. T., Dunlop I. E., Porter A. E., ACS. Appl. Mater. Inter., 2017, 9(45): 39259—39270
- [5] Zhong L., Zhai X. D., Zhu X. F., Yao P. P., Liu M. H., Langmuir, 2010, 26(8): 5876—5881
- [6] Feng J. J., Chen S. S., Chen X. L., Zhang X. F., Wang A. J., Colloid Interf. Sci., 2017, 509:73—81
- [7] Wang A. J., Qin S. F., Zhou D. L., Cai L. Y., Chen J. R.,

- Feng J. J., *Rsc. Adv.*, 2013, 3(34) :14766—14773
- [8] Jian Y. Y., Deng Z. J., Yang D., Deng X., Li Q., Sha Y. L., Li C. H., Xu D. S., *Nano Res.*, 2015, 8(7):2152—2161
- [9] Barbosa S., Agrawal A., Rodríguez-Lorenzo L., Alvarez-Puebla R. A., Komowski A., Weller H., Liz-Marzan L. M., *Langmuir*, 2010, 26(18) :14943—14950
- [10] Han J., Li J. R., Jia W. F., Yao L. M., Li X. Q., Jiang L., Tian Y., *Int. J. Nanomed.*, 2014, 9: 517—526
- [11] Kumari S., Singh R. P., *Int. J. Biol. Macromol.*, 2012, 50(3):878—883
- [12] Zhao L., Sun X., Ji X., Li J., Yang W., Peng X., *J. Phys. Chem. C*, 2009, 113:16645—16651
- [13] Mao K., Chen Y., Wu Z., Zhou X., Shen A., Hu J., *J. Agric. Food Chem.*, 2014, 62:10638—10645
- [14] Zhao X. M., Qi T. Y., Kong H. F., Hao M., Wang Y. Q., Li J., Liu B. C., Gao Y. Y., Jiang J. L., *Int. J. Nanomed.*, 2018, 13: 6413—6428
- [15] Liu Z. G., Qu S. X., Wen J., *Prog. Chem.*, 2015, 27(2/3) :212—219
- [16] Liu Y. W., Guo Z., *Chem. J., Chinese Universities*, 2015, 36(7) :1389—1394
- [17] Khlebtsov B. N., Burov A. M., Khlebtsov N. G., *Appl. Mater. Today*, 2019, 15:67—76
- [18] Jiang Y. Y., Wu X. J., Li Q., Li J. J., Xu D. S., *Nanotechnology*, 2011, 22(38) :385601
- [19] Luo Y. S., Ji X. H., Zhuang J. Q., Yang W. S., *Colloid Surface A*, 2014, 463:28—36
- [20] de Vries W. C., Niehues M., Wissing M., Wurthwein T., Masing F., Fallnich C., Studer A., Ravoo J. J., *Nanoscale*, 2019, 11(19): 9384—9391
- [21] Garrido C., Wsiss-Lopez B. E., Vallette M. M. C., *Spectrosc. Lett.*, 2016, 49(1):11—18
- [22] Chen W. F., Qin M., Chen X. Y., Wang Q., Zhang Z. R., Sun X., *Theranostics*, 2018, 8(8):2229—2241
- [23] Poinard B., Neo S. Z. Y., Yeo E. L. L., Heng H. P. S., Neoh K. G., Kah J. C. Y., *ACS Appl. Mater. Inter.*, 2018, 10(25):21125—21136
- [24] Fu J. W., Chen Z. H., Wang M. H., Liu S. J., Zhang J. H., Zhang J. N., Han R. P., Xu Q., *Chem. Eng. J.*, 2015, 259:53—61